Received: 21 May 2018 | Accepted: 2 September 2018

DOI: 10.1111/ane.13024

ORIGINAL ARTICLE

WILEY Acta Neurologica Scandinavica

Glucose metabolism in the brain in LMNB1-related autosomal dominant leukodystrophy

Johannes Finnsson[1] | Mark Lubberink[2] | Irina Savitcheva[2,4] | David Fällmar[1] | Atle Melberg[3] | Eva Kumlien[3] | Raili Raininko[1]

[1]Radiology, Uppsala University, Uppsala, Sweden

[2]Nuclear Medicine and PET, Uppsala University, Uppsala, Sweden

[3]Neuroscience, Neurology, Uppsala University, Uppsala, Sweden

[4]Clinical Science, Intervention and Technology (CLINTEC), Karolinska Institutet, Stockholm, Sweden

Correspondence
Raili Raininko, Radiology, Uppsala University, Uppsala, Sweden.
Email: Raili.Raininko@radiol.uu.se

Funding information
This study was supported by grants from the Ländell Foundation, Selander Foundation, Hedberg Foundation for Medical Research, and by the Swedish Medical Research Council Grants 73X-13158 and K2013-66X-10829-20-3.

Objective: *LMNB1*-related autosomal dominant leukodystrophy is caused by an overexpression of the protein lamin B1, usually due to a duplication of the *LMNB1* gene. Symptoms start in 5th to 6th decade. This slowly progressive disease terminates with death. We studied brain glucose metabolism in this disease using ^{18}F-fluorodeoxyglucose positron emission tomography (PET).

Methods: We examined 8 patients, aged 48-64 years, in varying stages of clinical symptomatology. Two patients were investigated with quantitative PET on clinical indications after which six more patients were recruited. Absolute glucose metabolism was analyzed with the PVElab software in 6 patients and 18 healthy controls. A semiquantitative analysis using the CortexID software was performed in seven investigations, relating local metabolism levels to global glucose metabolism.

Results: The clinical quantitative PET revealed low global glucose metabolism, with the most marked reduction in the cerebellum. In the PVElab analysis, patients presented low mean glucose metabolism in the cerebellum, brainstem and global grey matter. In the semiquantitative analysis, 2 patients showed a decreased metabolism in the cerebellum and 4 patients a relatively higher metabolism in parts of the temporal lobes. Since none of the patients showed an increased metabolism in the quantitative analysis, we interpret these increases as "pseudo-increases" related to a globally reduced metabolism.

Conclusions: Global reduction of grey matter glucose metabolism in this white matter disease most likely depends on a combination of cortical afferent dysfunction and, in later stages, neuronal loss. The lowest metabolism in the cerebellum is consistent with histopathological findings and prominent cerebellar symptoms.

KEYWORDS

^{18}F-fluorodeoxyglucose, adult-onset leukodystrophy, autosomal dominant leukodystrophy, glucose metabolism, positron emission tomography

1 | INTRODUCTION

LMNB1-related autosomal dominant leukodystrophy (ADLD) is an adult-onset disease in which the first symptoms manifest in the 5th to 6th decade.[1,2] The original report described the disease as a "hereditary adult-onset leukodystrophy simulating chronic progressive multiple sclerosis",[1] and in some later papers it has been called adult-onset ADLD with autonomic symptoms.[3,4] The disease is caused by an increased expression of the nuclear protein lamin B1, due to either a duplication of the *LMNB1* gene (OMIM #150340)[5-7] or enhancer adoption due to a genomic deletion.[8] The increased levels of lamin B1 seem to cause age-dependent inhibition of lipid synthesis in oligodendrocytes, resulting in demyelination.[9] Lamin B1 levels also modulate the development of neurons and astroglial-like cells.[10-13]

Patients most often present with autonomic dysfunction, later progressing with symptoms from cerebellum and spinal tracts, pseudobulbar signs, cognitive decline, and finally death, usually approximately two decades after symptom onset.[1,2,6] All patients seem to develop bladder dysfunction which is usually the first symptom. In about three quarters of the patients, orthostatic hypotension has been found.[2] From the cardiovascular point of view, the impairment of the autonomic control is limited to the sympathetic system.[14]

Typical magnetic resonance imaging (MRI) findings in the brain include early involvement of the cerebellar peduncles and corticospinal tracts progressing to symmetrical extensive cerebral white matter changes. The periventricular area is typically less affected. The spinal cord is abnormally thin with pathological signal intensity in the white matter. These findings, together with clinical symptoms of myelopathy with autonomic dysfunction, are sufficiently specific to enable the diagnosis, which can be confirmed by genetic analysis.[2,6]

On histological examinations, myelin appears rarefied and vacuolated. There is no significant pathology in the cerebral cortex, while in the cerebellum the number of Purkinje cells is reduced and the number of Bergmann astroglial cells slightly increased.[3] In studies using magnetic resonance spectroscopy, to investigate the metabolism in the white matter in patients with *LMNB1*-related ADLD, lactate has been found in the cerebrospinal fluid but not in the brain parenchyma. Further, metabolite levels in the parenchyma have been found to be normal when quantified using creatine as an internal reference.[15,16] There are no previous studies measuring glucose metabolism in *LMNB1*-related ADLD.

The aim of this study was to investigate glucose metabolism in the brain in *LMNB1*-related ADLD using ^{18}F-fluorodeoxyglucose positron emission tomography (FDG-PET).

2 | MATERIALS AND METHODS

2.1 | Subjects

Eight patients, aged 48-64 years, from two unrelated families segregating for two different *LMNB1* duplications were examined with quantitative FDG-PET of the brain. Patient details are presented in

TABLE 1 Patient characteristics and type of PET analysis

Patient No.	Age (y)	Sex	Family	Age at symptom onset and first symptoms	Clinical symptoms				EDSS	MRI	PET-analysis	
					Autonomic	Pyramidal	Cerebellar	Other		Grade[a]	Quantitative	Semiquantitative
1	64	F	1	51 Bladder symptoms, tremor	++	+	+	Parkinsonism	8	5	Y	Y
2	60	F	1	43 Bladder symptoms	++	+	++	–	7	5	Y[b]	N[b]
3	59	F	1	47 Bladder symptoms, gait difficulty	++	–	++	RA/iritis	3.5	4	Y	Y
4	57	F	1	43 Bladder symptoms	+++	++	+	–	4	3	Y	Y
5	57	M	2	40 Bladder symptoms, gait difficulty	+++	+++	+	–	9	5	Y	Y
6	51	M	2	43 Bladder symptoms, gait difficulty	+++	++	+	–	6	4	Y	Y
7	50	M	1	41 Bladder symptoms, gait difficulty	+++	++	+	–	6.5	4	N[c]	Y
8	48	M	1	47 Bladder symptoms, erectile dysfunction	++	+	+	–	3	3	Y	Y

RA, Rheumatoid arthritis; F, Female; M, Male; Y, Performed; N, Not performed.
EDSS, Kurtzke's expanded disability status scale: 3—Fully ambulatory; 6—Needs intermittent or unilateral constant assistance (cane, crutch or brace) to walk 100 metres; 7—Essentially restricted to wheelchair; 9—Confined to bed, can communicate and eat.
[a]MRI Grade, scale presented in ref (Finnsson et al. 2015)[2]. For examples of grades 3 and 5, please, see Figure 1.
[b]The original datasets were not available. Original clinical quantitative analysis used in the study.
[c]The blood sampling failed.

Table 1. All patients had pathological findings on MRI. Figure 1 exemplifies the findings in Patients 8 and 5, representing the mildest and most severe pathological MRI changes in this study. Patients 1 and 2 had been examined on clinical indications before the diagnosis of *LMNB1*-related ADLD was confirmed. Because of the rare findings of pronounced decreased glucose metabolism in the cerebellum, we were encouraged to recruit six more patients to investigate whether this was a consistent finding in the disease. Data from 18 healthy controls, aged 58-69 years, median and mean 64 years, were used for comparison in a quantitative analysis.

2.2 | FDG-PET technique

Patients 1 and 2 were examined according to a standard clinical protocol, using a dynamic scan with a start directly after intravenous injection of FDG and the following frame durations: 5 × 60 seconds, 5 × 180 seconds, 5 × 300 seconds, and 1 × 600 seconds. The scan time was 55 minutes. More details have been described in a previous publication.[17] Patient 1 was examined with a Siemens ECAT EXACT HR+ scanner (CTI PET Systems Inc., Knoxville, TN, USA) and Patient 2 with a GE 2048-15B Plus PET camera (General Electric Medical Systems, Uppsala, Sweden). Attenuation correction was performed using a 10-minute transmission scan with rotating ^{68}Ge rod sources.

Patients 3-8 and the controls were examined with a Discovery ST (GE Healthcare, USA) PET/CT scanner after injection of 3 MBq/kg FDG. In Patients 3, 5, 6, and 8, emission data acquisition started at the time of FDG injection, and the scan time was 45 minutes, with the following frame durations: 6 × 10 seconds, 3 × 20 seconds, 2 × 30 seconds, 2 × 60 seconds; 2 × 150 seconds, and 7 × 300 seconds. Blood sampling was performed at 15, 25, 35, 45, 60, and 90 seconds, and at 2, 3, 5, 7, 10, 20, 30, and 45 minutes. In Patients 4 and 7 and the controls, the scanning started 20 minutes after FDG injection, and the scan time was 25 minutes with frame durations 5 × 300 seconds. Blood sampling was performed at 45 seconds and 1, 2, 3, 5, 10, 20, 45, and 60 minutes. In all subjects, a heat pad was used to arterialize venous blood. Blood glucose levels were used to calculate absolute values for glucose metabolism in the brain. A low dose CT was performed in the same session for attenuation correction.

2.3 | Data analysis

In Patient 7, blood sampling failed and no quantitative data could be obtained. In Patients 1, 3-6, and 8 and in the controls, quantitative glucose metabolism images were produced by the method described by Patlak.[18] The data were post-processed using the software PVElab[19] and automatically divided into 46 volumes of interest (VOIs) using a probability-based method.[20] Forty-four of these 46 VOIs were bilateral and from these an average value of the two sides was calculated. Data from the three VOIs of the brainstem were also combined, leaving 22 VOIs plus the values of the global glucose metabolism.

In Patient 2, software post-processing could not be performed as the original data of the examination was no longer

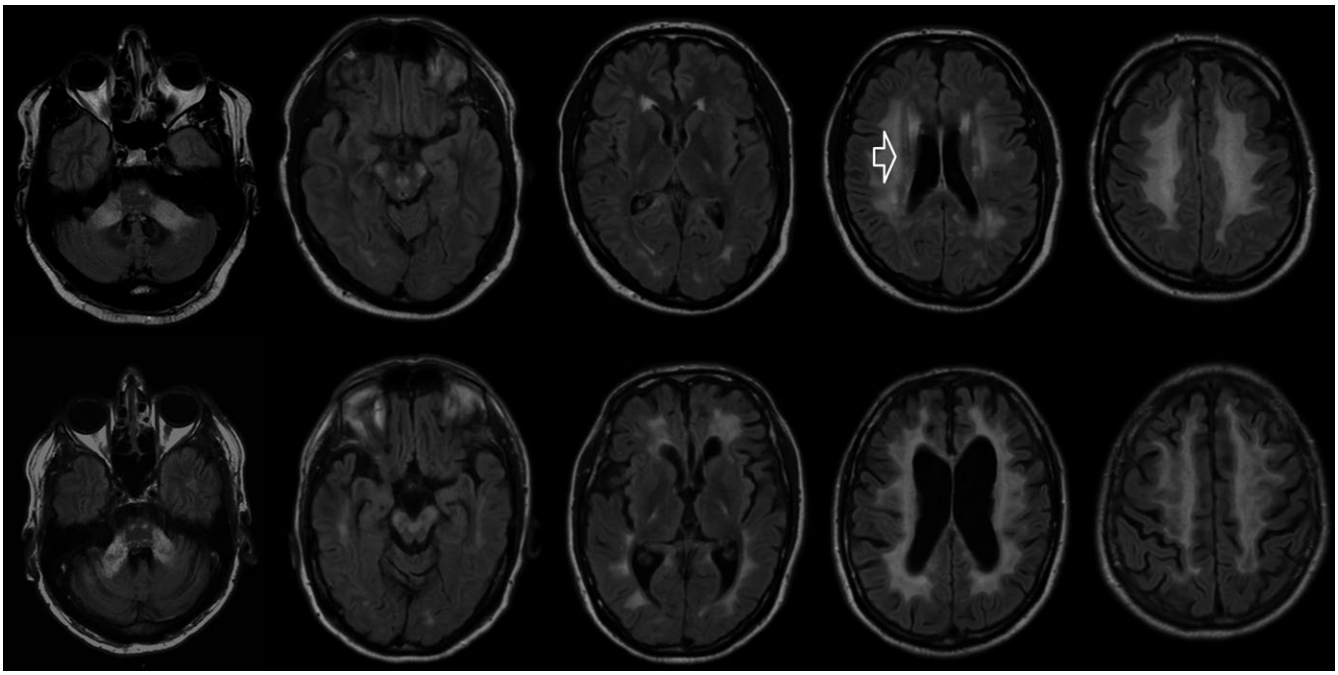

FIGURE 1 MR images of the least and most severely affected patients. Patient 8, top row, presenting MRI grade 3 changes with T2 hyperintensities in the cerebellar peduncles, along the corticospinal tracts and in the supratentorial white matter in the frontal, parietal, and occipital lobes. A less affected periventricular rim can be seen (arrow). Patient 5, bottom row, presenting grade 5 changes with extension of the white matter changes into the temporal lobes as well as enlargement of ventricles and sulci. T2-weighted fluid attenuation inversion recovery (FLAIR) sequence

extant. Quantitative FDG-PET data had been analyzed at the time of examination using Patlak analysis and manual delineation of cortical and subcortical VOIs as described in detail in a previous publication.[21]

FDG-PET data from Patients 1 and 3-8 were also analyzed semi-quantitatively with the software suite CortexID (GE Healthcare, Marlborough, MA, USA), using the standardized uptake value (SUV) of the whole brain as a reference and comparing the findings to a dataset of 140 age-matched healthy controls from the material provided by the manufacturer. The original dataset of Patient 2 was not extant and could not be analyzed using the CortexID software.

2.4 | Statistical analysis

Statistical analyses were performed using the free software R. Welch's unequal variance *t* tests were performed to find statistically significant differences in levels of FDG uptake and glucose metabolism. No correction for multiple comparisons was performed but the brain regions were tested separately.

The study was approved by the regional ethics committee and performed in accord with the ethical standards of the Declaration of Helsinki. Subjects gave informed consent before participating in the study.

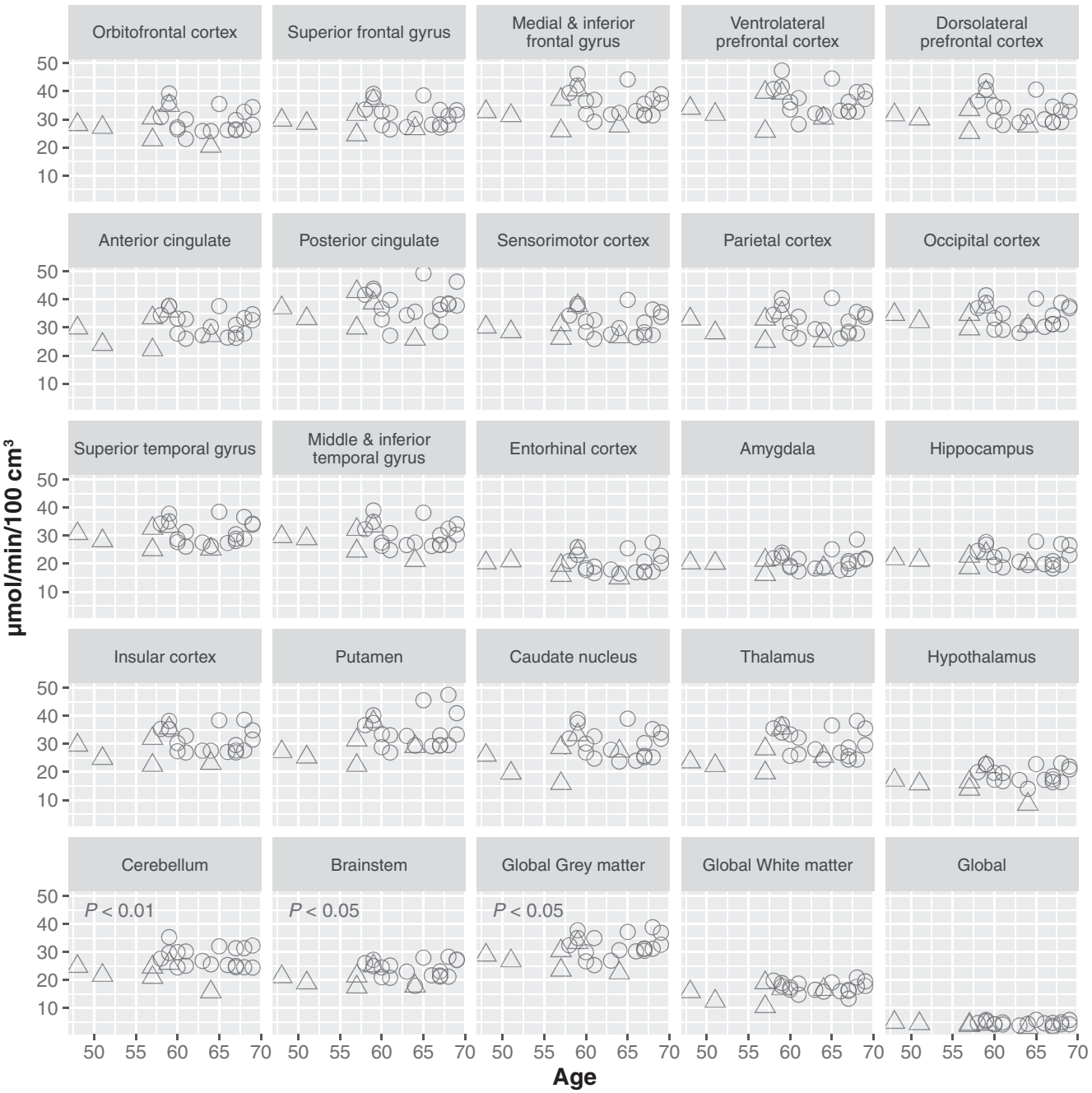

FIGURE 2 Glucose metabolism vs age by region of interest in patients (triangles) and healthy controls (dots) as analyzed with PVElab

3 | RESULTS

3.1 | Absolute glucose metabolism analyzed with PVElab in Patients 1, 3-6, and 8

Figure 2 presents glucose metabolism in individual VOIs as well as globally in patients and controls. There was a 16% reduction in mean uptake in the cerebellum ($P = 0.0098$), a 15% reduction in the brainstem ($P = 0.027$), and a 14% reduction in the grey matter globally ($P = 0.043$). No significant difference in mean uptake was found in any other region. Patient 1, the oldest patient to be investigated, had significantly (> 2 SD) lower glucose metabolism in 5 of 22 VOIs (cerebellum, orbitofrontal cortex, medial and inferior frontal gyrus, middle and inferior temporal gyrus, posterior cingulate cortex, and hypothalamus), and in the grey matter globally. Glucose metabolism in Patient 5 (Figure 3), who was clinically most severely affected, with the most pronounced findings on MRI, was significantly lower in nine VOIs (brainstem, cerebellum, thalami, putamina, caudate nuclei, insular cortex, medial and inferior frontal gyrus, anterior cingulate cortex, and ventrolateral prefrontal cortex) as well as in the grey and white matter globally. Patient 6 had significantly lower metabolism in the caudate nuclei and global white matter compared to the controls.

3.2 | Quantitative analysis in patient 2

Patient 2 had approximately 30% or 1.9 SD lower global glucose metabolism compared to normal values, with the cerebellum showing the most marked reduction, approximately 45% or 2.2 SD lower than normal values.

3.3 | Semiquantitative glucose metabolism of Patients 1 and 3-8 analyzed with CortexID

Regions of interest with statistically decreased or increased FDG uptake compared to the general FDG uptake (z-scores <−2 or > 2, respectively) are presented in Table 2. In Patients 1, 5, 6, and 8 a higher metabolism was found in parts of the temporal lobes compared to the global metabolism. In Patients 1 and 7, a decreased metabolism was seen in the cerebellum.

4 | DISCUSSION

In this study with FDG-PET, we found a reduced mean glucose metabolism in the cerebellum, brainstem, and global grey matter in patients with *LMNB1*-related ADLD. The lowest metabolism in the cerebellum is consistent with the clinical cerebellar symptoms as well as the MRI finding of early and pronounced changes in the middle cerebellar peduncles.[2] In addition, they are compatible with the earlier reported histopathological findings of a reduction of Purkinje cells and increase of Bergmann astroglial cells in the cerebellar cortex in this disease.[3]

Four of seven patients analyzed with a semiquantitative method had a higher relative glucose metabolism in the temporal lobes compared to global metabolism. However, since none of the patients showed an increased metabolism in the quantitative analysis, we interpret these findings as "pseudo-increases" related to a globally reduced metabolism. This is of importance for interpreting semiquantitative values in relation to the choice of reference region. The relatively higher temporal metabolism is in line with the evolution of MRI findings since the white matter of the temporal lobes is the last white matter area to be affected in LMNB1-related ADLD.[2]

Previously, 10 studies or case reports describing FDG-PET findings in a total of 21 patients with leukodystrophies have been reported.[22-31] Seventeen of these patients had X-linked adrenoleukodystrophy (X-ALD), including adrenomyeloneuropathy (AMN). As glucose metabolism is physiologically much higher in grey than in white matter, metabolic changes on FDG-PET could be mainly found in grey matter, whereas abnormal FDG uptake in white matter was only described in three of those 21 patients.[23,24,26] We found a significantly abnormal uptake in two of our eight patients in global white matter but there was no significant difference between the patients and the controls as groups. Brain regions with reduced glucose metabolism were found in all leukodystrophy patients both in literature and in our study. In X-ADL, increased metabolic activity was also detected.[24,31] In addition to the cortical areas overlying pathological white matter, analysis of brain glucose metabolism could reveal abnormalities in regions without signal changes on MRI[22,32] and, in AMN patients, even with a totally normal MRI.[29,31] In contrast, no abnormal glucose metabolism could be found in the vicinity of some white matter changes on MRI in 1 patient.[31] In the only previous multi-subject PET study on leukodystrophy,[31] a characteristic pattern was found for X-ALD: hypermetabolism in the frontal areas and anterior cingulate cortex and hypometabolism in the temporal areas and cerebellum.

The physiopathological basis of the reduced cortical glucose metabolism in leukodystrophies is not known but it has been hypothesized that hypometabolism in X-ADL is not due to true pathological changes in these areas but to altered connectivity, deafferentation, in white matter.[30,31] This hypothesis was supported by the lack of cortical atrophy in affected locales on MRI. Postmortem studies of X-ALD have also not shown any atrophy.[32] The increased levels of lamin B1 do not only affect oligodendrocytes and, secondarily to that, myelin[9] but also neuronal development.[10-12] However, in histopathological studies of patients with *LMNB1*-related ADLD, the cerebral cortex has been normal.[3,33] Therefore, we assume that the globally decreased glucose metabolism in the cerebral cortex in *LMNB1*-related ADLD can mainly be secondary to myelin vacuolization and loss, consistent with the extensive T2 hyperintensities seen on MRI, causing decreased functioning of the axons connecting different cortical areas and deep grey matter structures. However, given the level of atrophy presented by patients with *LMNB1*-related ADLD in advanced stages, exemplified in Figure 1, it is plausible that some neuronal loss occurs in the cortex, and the decreased global metabolism

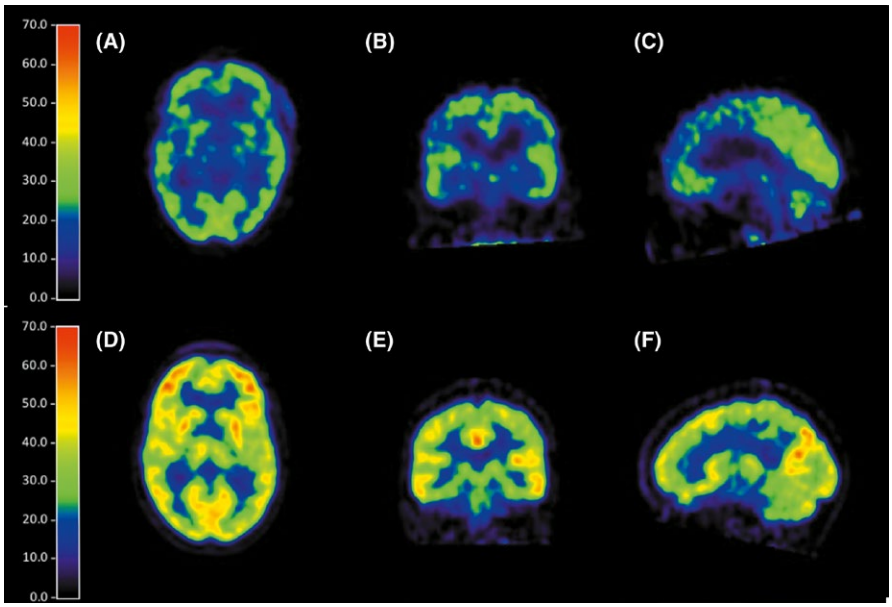

FIGURE 3 FDG-PET images of the most severely affected patient (Patient 5, A-C) compared with a healthy control (D-F). Axial (A, D), coronal (B, E), and sagittal (C, F) images showing decreased glucose metabolism in the patient

TABLE 2 Regions with glucose metabolism lower or higher than globally in the brain in the semiquantitative analysis with the CortexID software suite

Patient	Areas with *z*-score <−2	Areas with *z*-score >2
1	L Prefrontal lateral [−2.44] R Posterior cingulate [−3.08] R Parietal inferior [−2.34] Cerebellum [−2.10]	L Occipital lateral [+2.44] L Temporal mesial [+2.10]
3	L Precuneus [−3.36]	None
4	None	None
5	R Prefrontal lateral [−3.01] R Anterior cingulate [−3.00] L Anterior cingulate [−3.48]	L Occipital lateral [+2.52] L Temporal lateral [+2.25] R Temporal mesial [+2.72] L Temporal mesial [+2.73]
6	L Anterior cingulate [−2.01]	L Occipital lateral [+2.05] R Temporal lateral [+3.95] L Temporal lateral [+2.21] R Temporal mesial [+2.36]
7	Cerebellum [−3.59] Pons [−3.29]	R Prefrontal lateral [+2.68] R Parietal inferior [+2.17]
8	None	R Precuneus [+2.25] R Parietal superior [+2.56] R Temporal lateral [+2.63]

z-score, standard score (number of standard deviations from the mean); L, left; R, right.

might be due to a combination of axonal dysfunction and neuronal loss. Deafferentation most likely also influences in the cerebellum but, in the cerebellar cortex, even histopathological abnormalities have been described.[3] This is consistent with the lowest glucose uptake in the cerebellum. Increased glucose metabolism, only described in X-ALD, might be a sign of increased activity of neuronal cells in response to disconnection as speculated by Salsano et al[31] It may also correspond to the active neuroinflammatory process in X-ALD.[34]

The age matching between the patients and control group is not optimal in the quantitative part of this study. For ethical reasons, we could not recruit age-matched controls for a PET study. However, as cerebral glucose metabolism decreases with age[35] and the patients were on average 10 years younger than the controls, we believe we can trust the findings of decreased glucose metabolism in the patients. Our most severely affected patient was 7 years younger than the average age of the controls.

In conclusion, in patients with *LMNB1*-related ADLD, mean glucose metabolism is decreased in the cerebellum, brainstem and global grey matter. The cerebellar findings are consistent with clinical cerebellar symptoms, MRI findings, and histopathology. The global reduction of glucose metabolism most likely depends on a combination of cortical afferent dysfunction and neuronal loss although a direct effect to neuronal cells cannot be excluded.

ACKNOWLEDGEMENTS

We thank the patients and families for their cooperation and participation in this study. We also thank the healthy volunteers for their participation.

CONFLICT OF INTEREST

There are no conflicts of interests to declare.

ORCID

Raili Raininko http://orcid.org/0000-0002-6897-7593

REFERENCES

1. Eldridge R, Anayiotos CP, Schlesinger S, et al. Hereditary adult-onset leukodystrophy simulating chronic progressive multiple sclerosis. *N Engl J Med*. 1984;311:948-953.
2. Finnsson J, Sundblom J, Dahl N, Melberg A, Raininko R. LMNB1-related autosomal-dominant leukodystrophy: clinical and radiological course. *Ann Neurol*. 2015;78:412-425.
3. Melberg A, Hallberg L, Kalimo H, Raininko R. MR characteristics and neuropathology in adult-onset autosomal dominant leukodystrophy with autonomic symptoms. *AJNR Am J Neuroradiol*. 2006;27:904-911.
4. Sundblom J, Melberg A, Kalimo H, Smits A, Raininko R. MR imaging characteristics and neuropathology of the spinal cord in adult-onset autosomal dominant leukodystrophy with autonomic symptoms. *AJNR Am J Neuroradiol*. 2009;30:328-335.
5. Padiath QS, Saigoh K, Schiffmann R, et al. Lamin B1 duplications cause autosomal dominant leukodystrophy. *Nat Genet*. 2006;38:114-1123.
6. Meijer IA, Simoes-Lopes AA, Laurent S, et al. A novel duplication confirms the involvement of 5q23.2 in autosomal dominant leukodystrophy. *Arch Neurol*. 2008;65:1496-1501.
7. Schuster J, Sundblom J, Thuresson A-C, et al. Genomic duplications mediate overexpression of lamin B1 in adult-onset autosomal dominant leukodystrophy (ADLD) with autonomic symptoms. *Neurogenetics*. 2011;12:65-72.
8. Giorgio E, Robyr D, Spielmann M, et al. A large genomic deletion leads to enhancer adoption by the lamin B1 gene: a second path to autosomal dominant adult-onset demyelinating leukodystrophy (ADLD). *Hum Mol Genet*. 2015;24:3143-3154.
9. Rolyan H, Tyurina YY, Hernandez M, et al. Defects of lipid synthesis are linked to the age-dependent demyelination caused by lamin B1 overexpression. *J Neurosci*. 2015;35:12002-12017.
10. Bartoletti-Stella A, Gasparini L, Giacomini C, et al. Messenger RNA processing is altered in autosomal dominant leukodystrophy. *Hum Mol Genet*. 2015;24:2746-2756.
11. Giacomini C, Mahajani S, Ruffilli R, et al. Lamin B1 protein is required for dendrite development in primary mouse cortical neurons. *Mol Biol Cell*. 2016;27:35-47.
12. Majahani S, Giacomini C, Marinaro F, et al. Lamin B1 levels modulate differentiation into neurons during embryonic corticogenesis. *Sci Rep*. 2017;7:4897.
13. Lo Martire V, Alvente S, Bastiniani S, et al. Mice overexpressing lamin B1 in oligodendrocytes recapitulate the age-dependent motor signs, but not the early autonomic cardiovascular dysfunction of autosomal-dominant leukodystrophy (ADLD). *Exp Neurol*. 2018;301:1-12.
14. Terlizzi R, Calandra-Buonaura G, Zanigni S, et al. A longitudinal study of a family with adult-onset autosomal dominant leukodystrophy: clinical, autonomic and neuropsychological findings. *Auton Neurosci*. 2016;195:20-26.
15. Finnsson J, Melberg A, Raininko R. ^{1}H-MR spectroscopy of adult-onset autosomal dominant leukodystrophy with autonomic symptoms. *Neuroradiology*. 2013;55:933-939.
16. Zanigni S, Terlizzi R, Tonon C, et al. Brain magnetic resonance metabolic and microstructural changes in adult-onset autosomal dominant leukodystrophy. *Brain Res Bull*. 2015;117:24-31.
17. Klunk WE, Engler H, Nordberg A , et al. Imaging brain amyloid in Alzheimer´s disease with Pittsburgh Compound-B. *Ann Neurol*. 2004;55:306-319.
18. Patlak CS, Blasberg RG, Fenstermacher JD. Graphical evaluation of blood-to-brain transfer constants from multiple-time uptake data. *J Cereb Blood Flow Metab*. 1983;3:1-7.
19. Quarantelli M, Berkouk K, Prinster A, et al. Integrated software for the analysis of brain PET/SPECT studies with partial-volume-effect correction. *J Nucl Med*. 2004;45:192-201.
20. Svarer C, Madsen K, Hasselbalch SG, et al. MR-based automatic delineation of volumes of interest in human brain PET images using probability maps. *NeuroImage*. 2005;24:969-979.
21. Engler H, Santillo AF, Wang SX, et al. In vivo amyloid imaging with PET in frontotemporal dementia. *Eur J Nucl Med Mol Imaging*. 2008;35:100-106.
22. Volkow ND, Patchell L, Kulkarni MV, Reed K, Simmons M. Adrenoleukodystrophy: imaging with CT, MRI, and PET. *J Nucl Med*. 1987;28:524-527.
23. Iinuma K, Haginoya K, Handa I, et al. Computed tomography, magnetic resonance imaging, positron emission tomography and evoked potentials at early stage of adrenoleukodystrophy. *Tohoku J Exp Med*. 1989;159:195-203.
24. Bakheet S, Al-Essa M, Patay Z, et al. Cerebral fluorine-18 fluorodeoxyglucose positron emission tomographic findings in x-linked adrenoleukodystrophy. *Clin Nucl Med*. 1999;24:364-365.
25. Salmon E, Van der Linden M, Maerfens Noordhout A, et al. Early thalamic and cortical hypometabolism in adult-onset dementia due to metachromatic leukodystrophy. *Acta Neurol Belg*. 1999;99:185-188.
26. Sawaishi Y, Hatazawa J, Ochi N, et al. Positron emission tomography in juvenile Alexander disease. *J Neurol Sci*. 1999;165:116-120.
27. Al-Essa MA, Bakheet SM, Patay ZJ, Powe JE, Ozand PT. Clinical and cerebral FDG PET scan in a patient with Krabbe's disease. *Pediatr Neurol*. 2000;22:44-47.
28. Johannsen P, Ehlers L, Hansen HJ. Dementia with impaired temporal glucose metabolism in late-onset metachromatic leukodystrophy. *Dement Geriatr Cogn Disord*. 2001;12:85-88.
29. Renard D, Castelnovo G, Collombier L, Kotzki P-O, Labauge P. Brain fludeoxyglucose F 18 positron emission tomography hypometabolism in magnetic resonance imaging–negative x-linked adrenoleukodystrophy. *Arch Neurol*. 2011;68:1338-1339.
30. Kim JE, Choi KG, Jeong JH, Kang HJ, Kim HS. Diffuse cortical hypometabolism on (18)F-FDG-PET scan in a case of an adult variant cerebello-brainstem dominant form of ALD manifesting dementia. *Parkinsonism Relat Disord*. 2012;18:210-212.
31. Salsano E, Marotta G, Manfredi V, et al. Brain fluorodeoxyglucose PET in adrenoleukodystrophy. *Neurology*. 2014;83:981-989.
32. Schaumburg HH, Powers JM, Raine CS, Suzuki K, Richardson EP. Adrenoleukodystrophy, a clinical and pathological study of 17 cases. *Arch Neurol*. 1975;32:577-591.
33. Coffeen CM, McKenna CE, Koeppen AH, et al. Genetic localization of an autosomal dominant leukodystrophy mimicking chronic progressive multiple sclerosis to chromosome 5q31. *Hum Mol Genet*. 2000;9:787-793.

34. Kumar A, Chugani KT, Chakraborty P, Huq AHMM. Evaluation of neuroinflammation in X-linked adrenoleukodystrophy. *Pediatr Neurol*. 2011;44:143-146.
35. Willis MW, Ketter TA, Kimbrell TA, et al. Age, sex and laterality effects on cerebral glucose metabolism in healthy adults. *Psychiatry Res*. 2002;114:23-37.

How to cite this article: Finnsson J, Lubberink M, Savitcheva I, et al. Glucose metabolism in the brain in LMNB1-related autosomal dominant leukodystrophy. *Acta Neurol Scand*. 2019;139:135-142. https://doi.org/10.1111/ane.13024